Nowe idee w fotowoltaice

A. Kołodziej

Third Generation Photovoltaic's

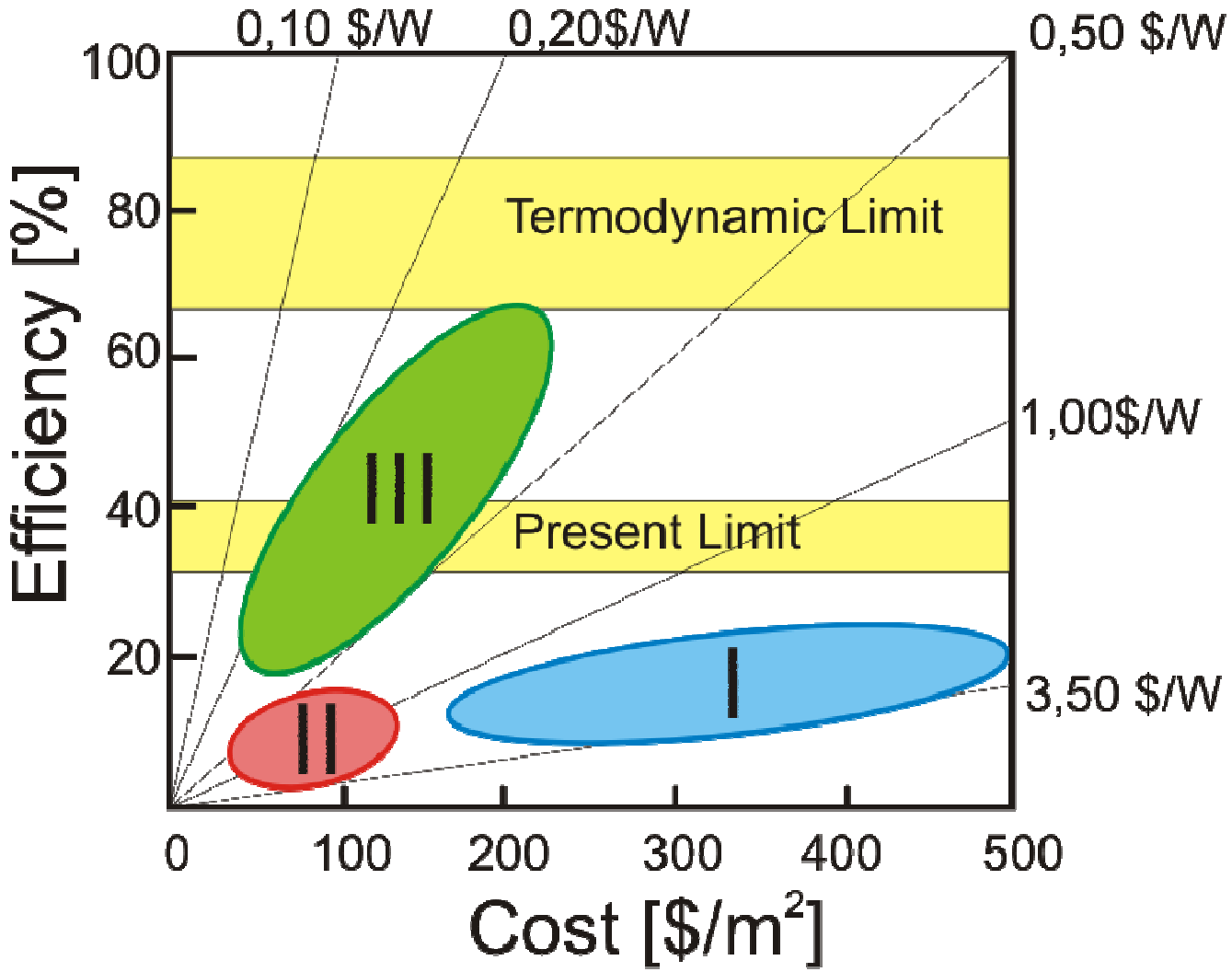

Third Generation Photovoltaic's

1. Sub bandgap losses
2. Lattice thermalisation

Two major losses – 60 %

Also:
3. Junction loss
4. Contact loss
5. Recombination

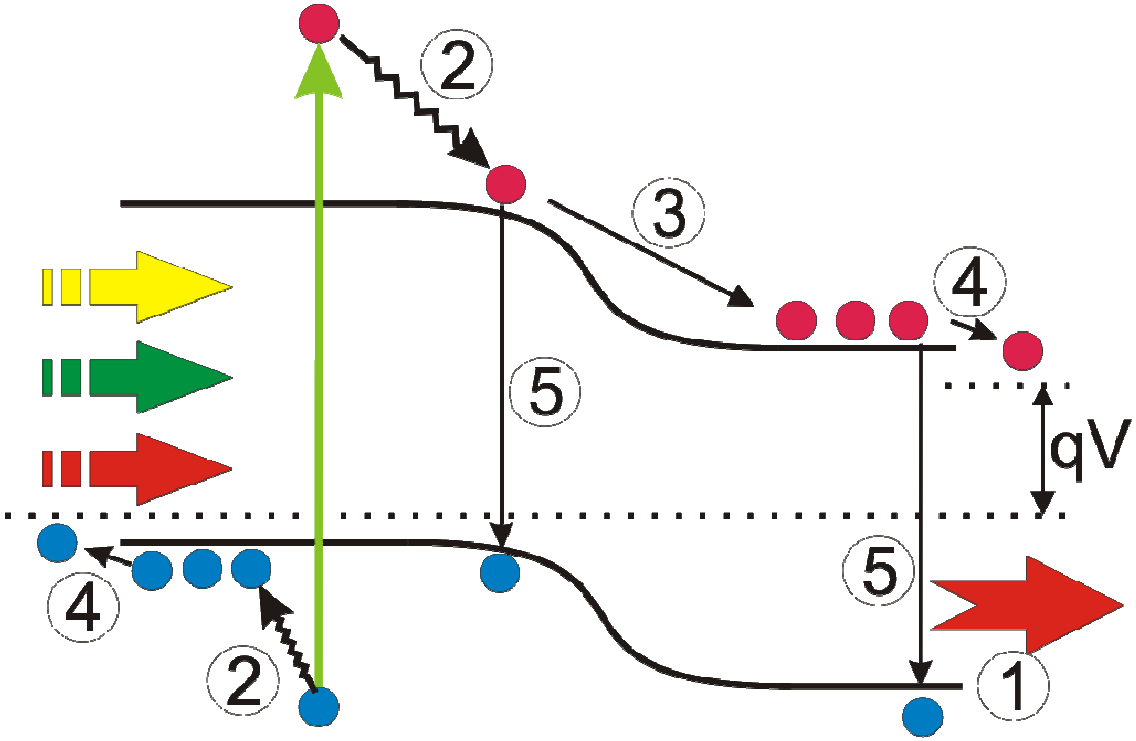

Limiting Efficiencies	1 sun
Single p-n junction:	31%
Multiple threshold:	68,2%

The Shockley – Queisser limit

Upper limit for homo – junction efficiency: 33%
Where do the remaining 67 % go ?

Termalization ($E > E_G$)	47%
Transmission ($E < E_G$)	18,5%l
Recombination	1,5%
Remaining efficiency	33%
Total	100%

M.C. Beard et al., Nano Letters 7 (2007) p. 2506

Third Generation Photovoltaic's

Solar cell concepts connected with quantum solution that allow for a more efficient utilization of the sunlight than homo – junction solar cells.

Main approaches:

- Modification of the photonic energy distribution prior to absorption in a front and back of solar cell
- Utilization of materials or cell structures incorporating several band gaps
- Reducing losses due to thermalization
  - Hot carrier solar cells
  - Impact ionization solar cells(down conversion)

Silicon based Tandem Cell

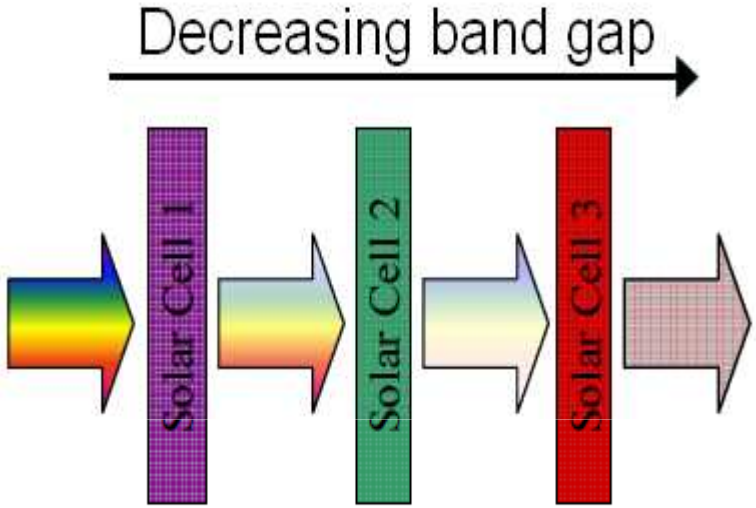

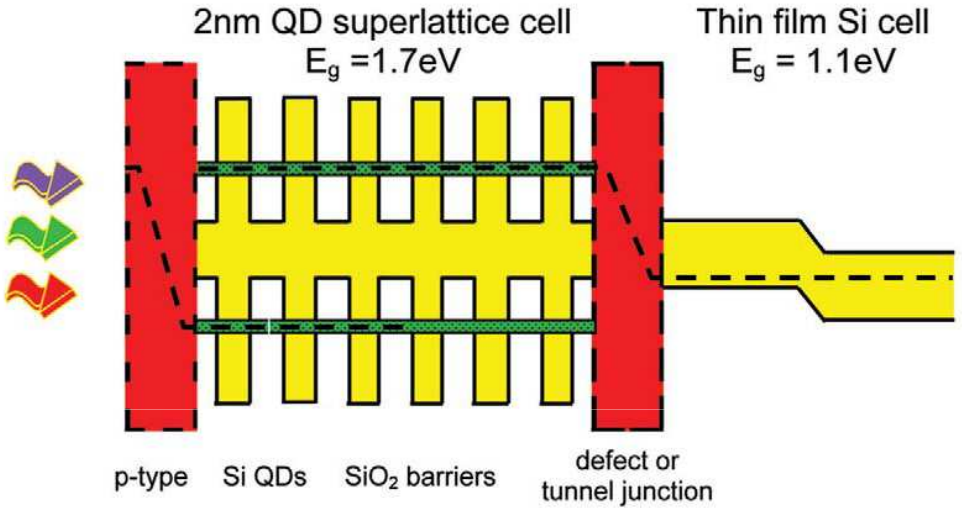

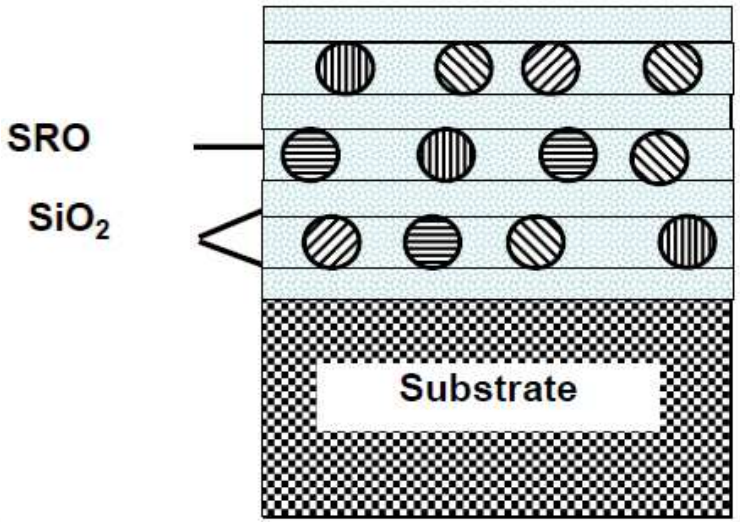

Engineer a wider band gap – Si QDs

Anneal 1100 °C – Si precipitation

$$SiO_x \rightarrow \frac{x}{2} SiO_2 + \left(1 - \frac{x}{2}\right) \cdot Si$$

Silicon nanostructure tandem cell

Alternate matrices

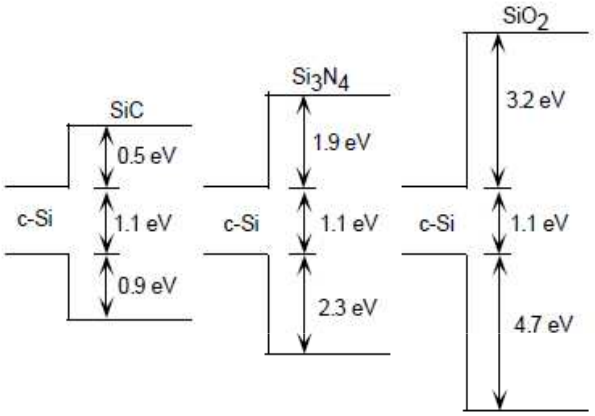

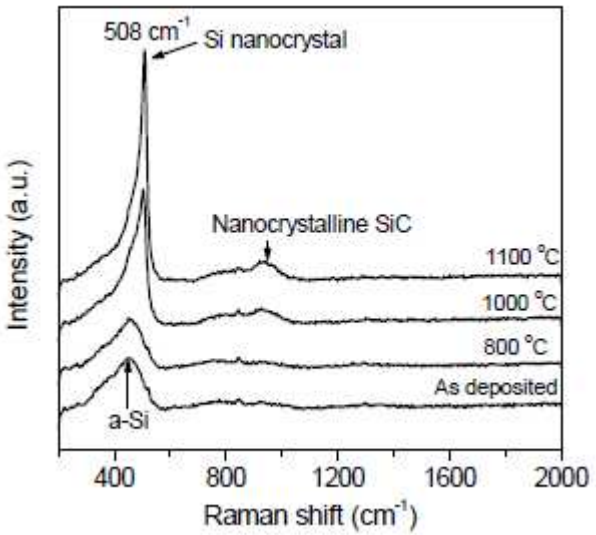

Si QDs in SiC

Si QDs in oxide/nitride

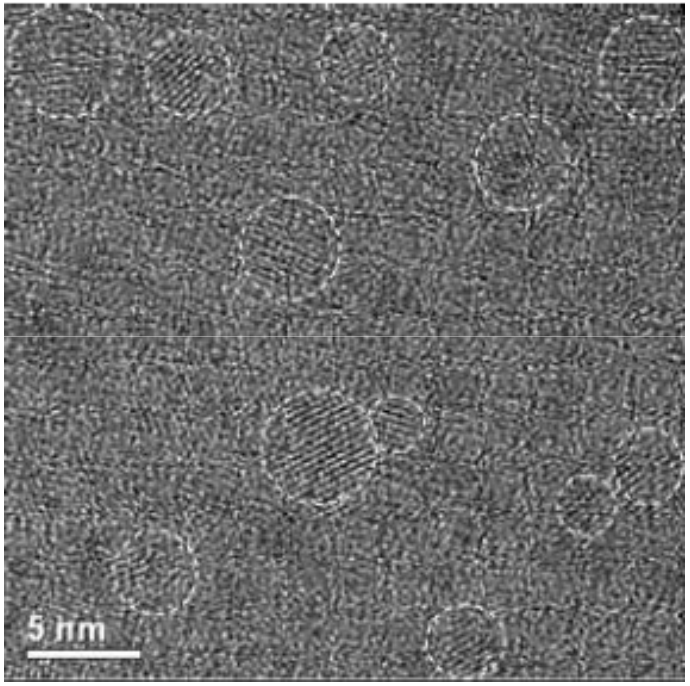

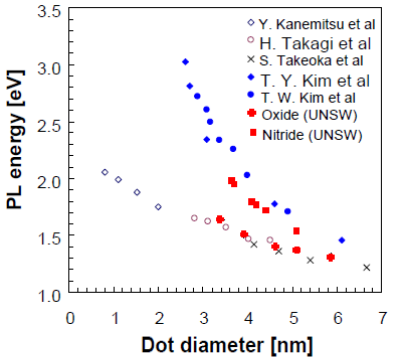

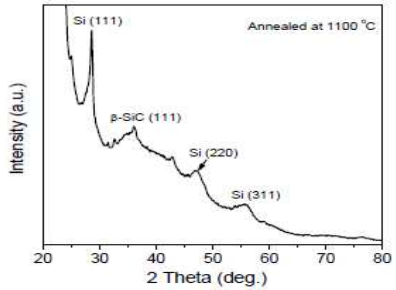

Fabrication of Si quantum dots

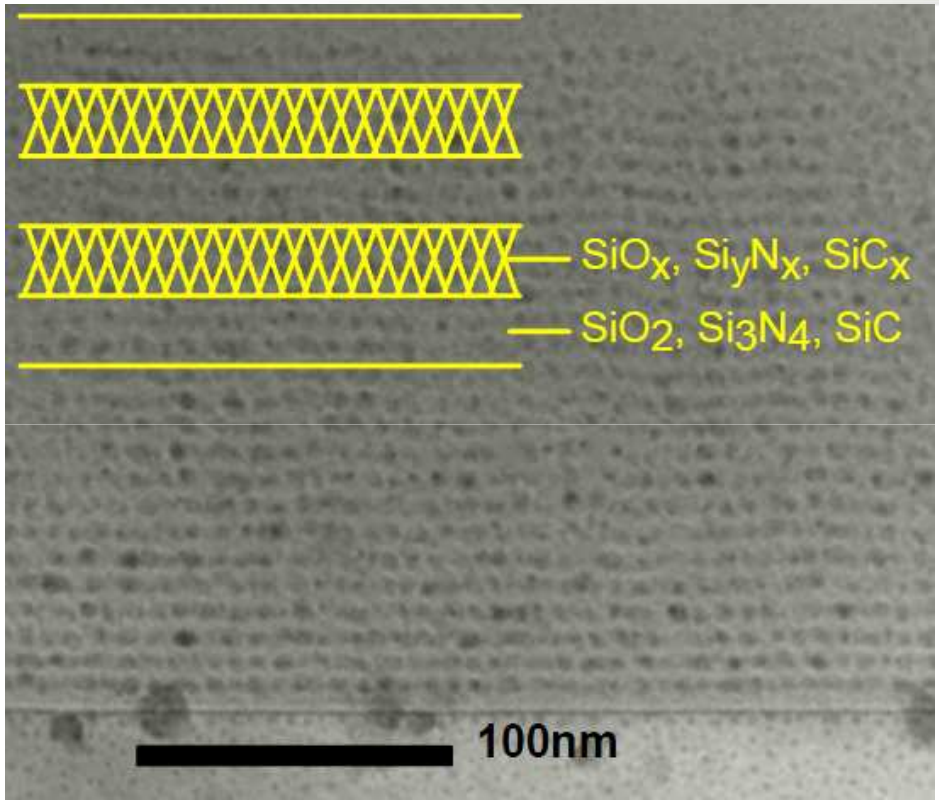

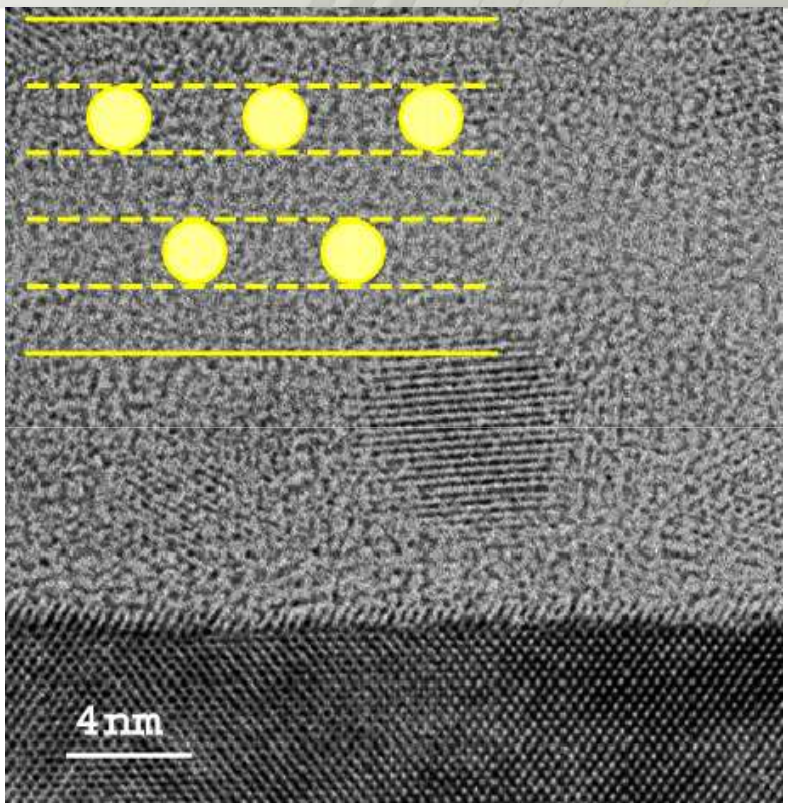

Zacharias et al., APL 80, 661, 2002

Fabrication of Si quantum dots

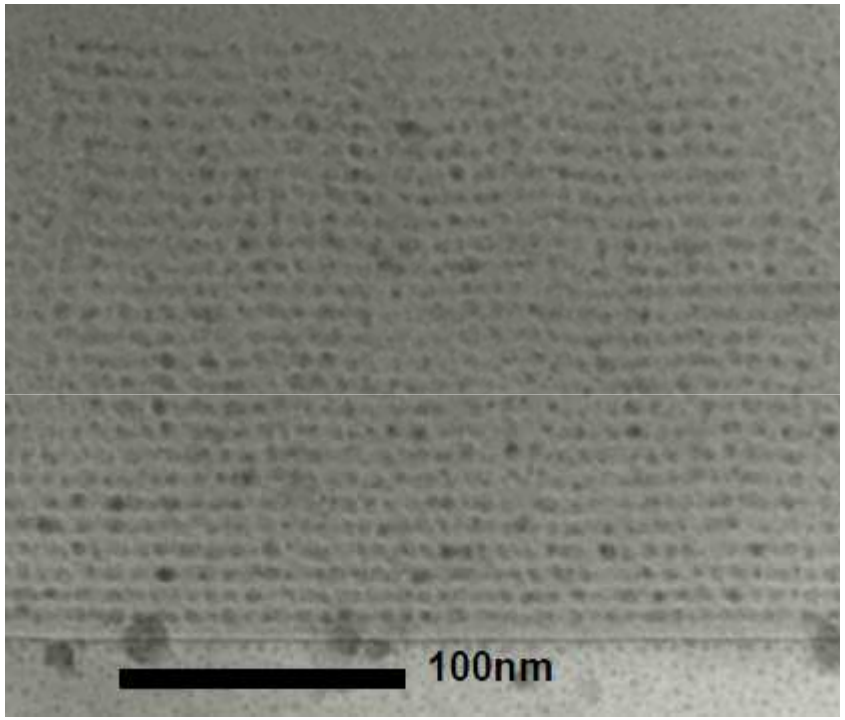

Nirm. PL. Spectra (2-5 nm dots; 300K)

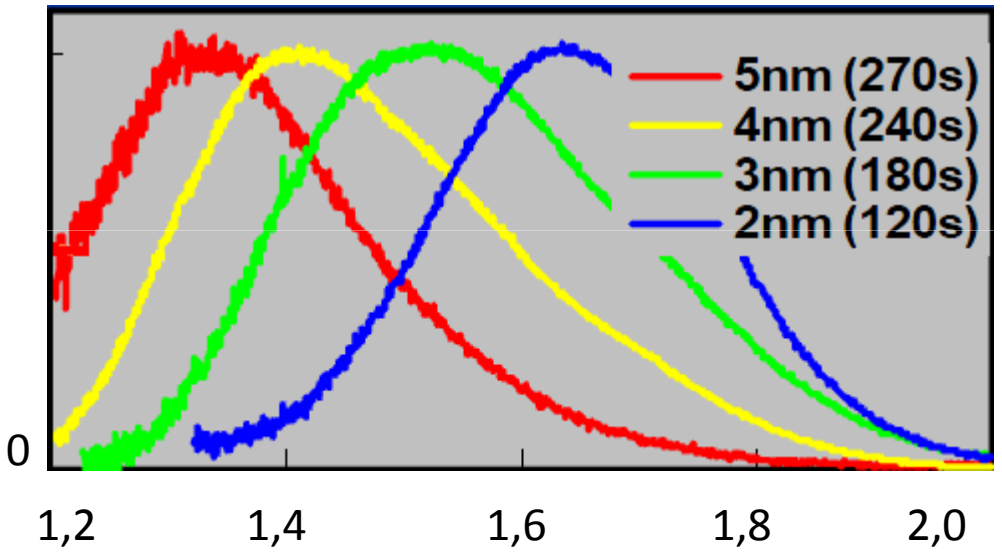

Improvement of energy conversion efficiency of amorphous silicon thin-film solar cells through plasmon effect

(1) CEA , Grenoble, France
(2) MANTIS, 2 Goodson Industrial Mews, United Kingdom
(3) Delft University of Technology, Photovoltaic Materials and Devices, The Netherlands
(4) Faculty of Electrical Engineering, University of Ljubljana, Ljubljana, Slovenia
(5) SOLARONIX, Switzerland
(6) ARC Photovoltaics Centre of Excellence, University of New South Wales, Australia

The 2-year **FP7 SOLAMON** project started in February 2009 aims at enhancing the absorption in several types of thin-film solar cells (amorphous thin film silicon, organic) through the surface plasmon effect generated by metallic nanoparticles, with a focus on a-Si:H solar cells.

Plazmony: metoda na pokonanie granicy dyfrakcyjnej

Miniaturyzacja światłowodow dielektrycznych jest ograniczona przez dyfrakcję do rozmiarow rzędu długości fali

- Wykorzystanie plazmonów pozwala pokonać granicę dyfrakcyjną, co umożliwia miniaturyzację układów fotonicznych
- Mikrofotografia: światło propagujące się w światłowodzie plazmonowym tj.w matrycach nano-cząstek „polem bliskim' zamiast w klasycznych światłowodach
- Centralnym problem problemem fotoniki (nano-optyki) jest dostarczenie, a następnie skoncentrowanie (nano-ogniskowanie) energii fali świetlnej . A plazmony pozwalają zogniskować i skoncentrować energię fali świetlnej w nanoskali w dwoch i trzech wymiarach

Niezwykła transmisja światła przez nanodziurki

Wywiercenie pojedynczej dziurki otoczonej centrycznymi rowkami umożliwia zgromadzenie enegii pola i jej przelanie przez dziurkę dzięki sprzężeniu plazmonu powierzchni przedniej i tylnej

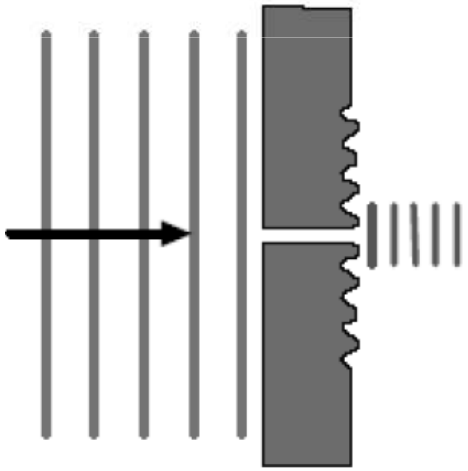

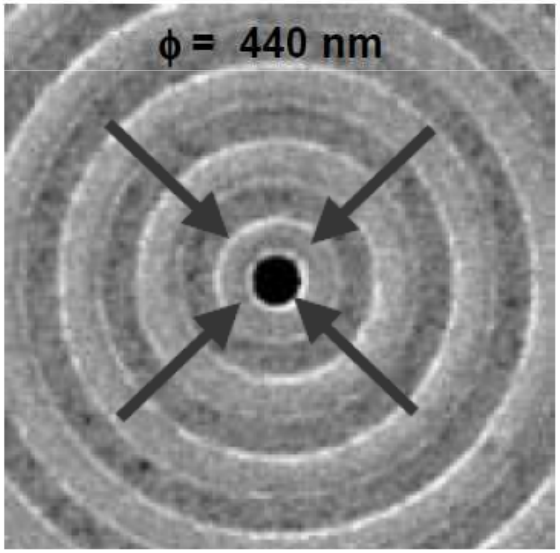

zmiana parametrów geometrycznych struktury pozwala sterować:
szerokością wiązki, kierunkiem wiązki ,długością fali rezonansowej

Zastosowania plazmonów

Liniowa i dwu wymiarowa matryca kulek na powierzchni

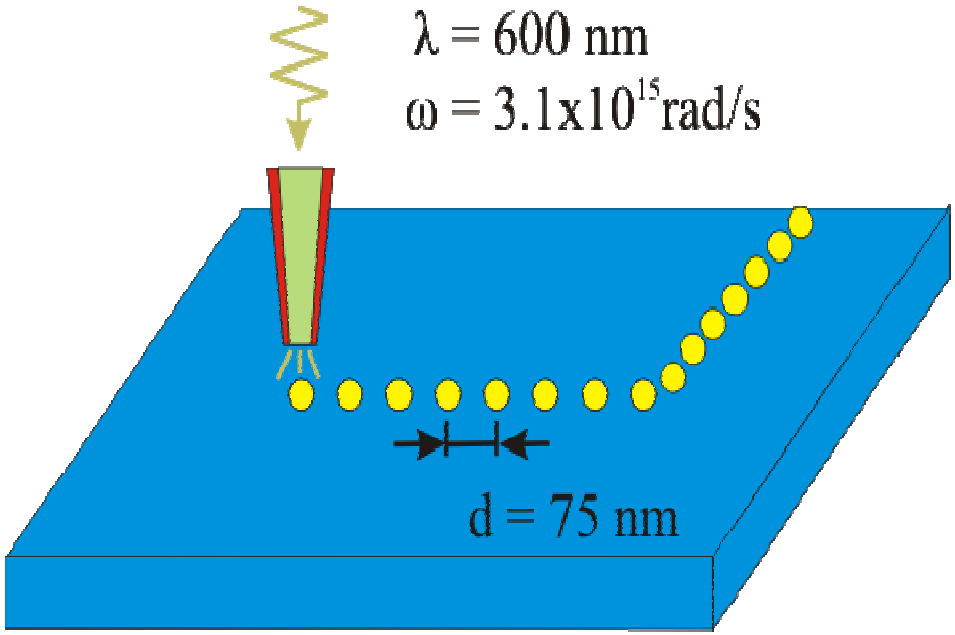

Światłowód

Elektroda frontowa
ogniwa słonecznego

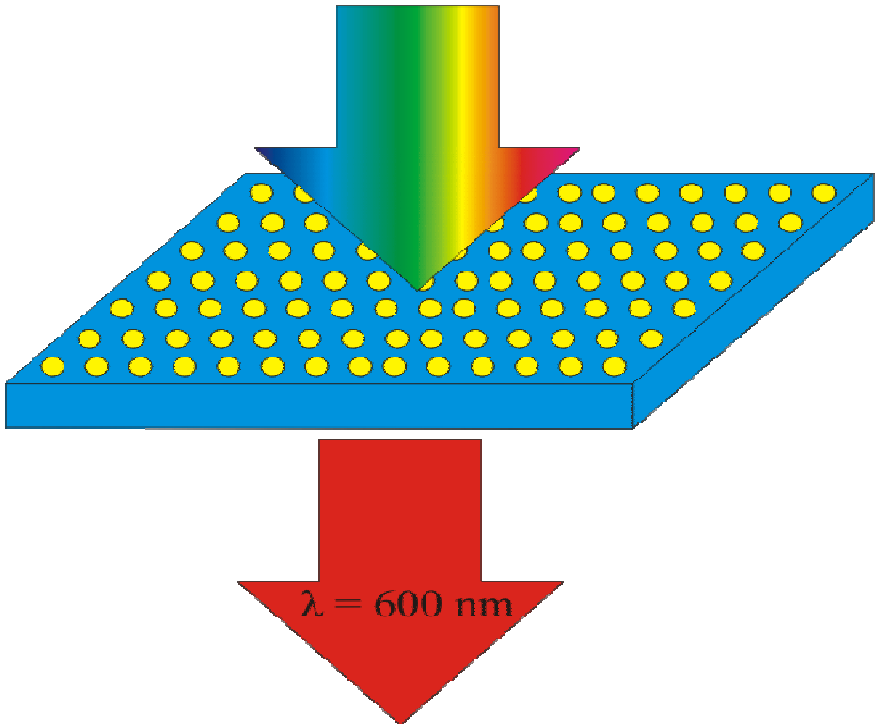

Maximum path length enhancement

Geometric series

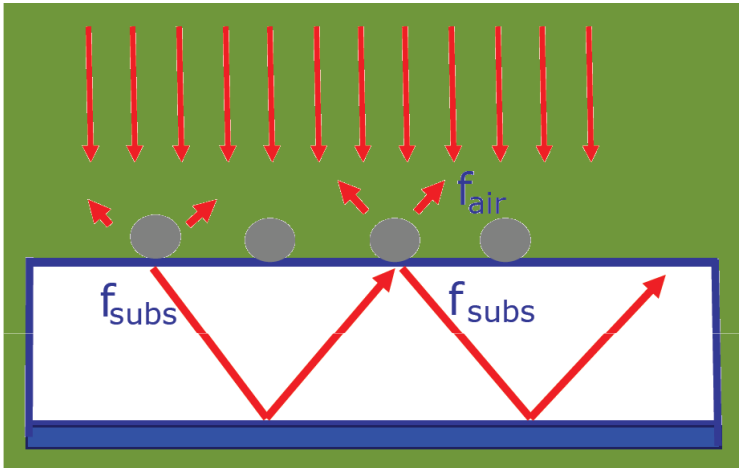

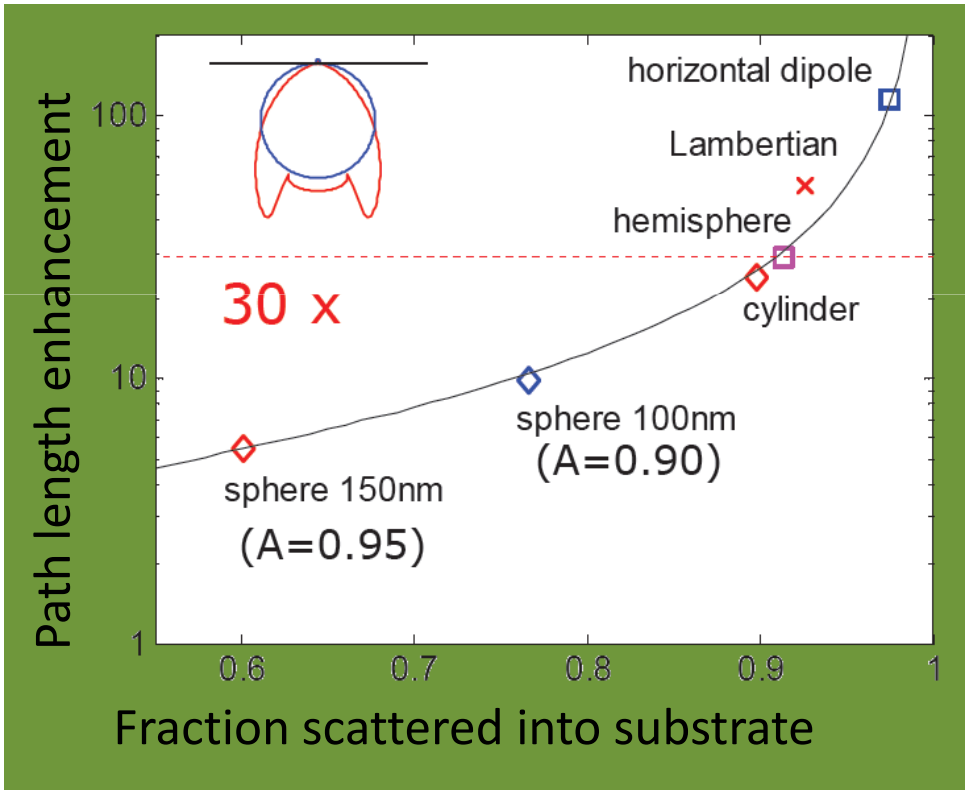

Highest path length enhancement for cylinder and hemisphere

Kylie Catchpole

Appl. Phys. Lett. **93, 191113 (2008), Opt. Expr. 16, 21793 (2008)**

Plasmonic solar cells,

K.R. Catchpole, and A. Polman,

(a) Radiation patterns for a point dipole oriented parallel to the surface at a distance of 20 nm from a Si substrate (blue dashed line). The radiation pattern for the case of free space is shown for reference (black solid line). b) Radiation patterns for a parallel point dipole 20 nm (blue dashed line) and 60 nm (red solid line) from a Si substrate.

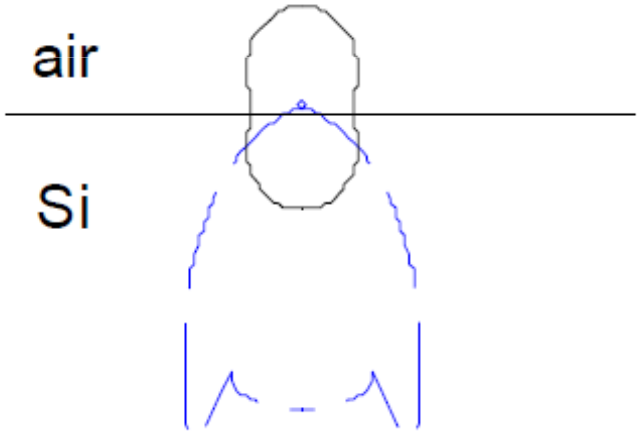

(a)

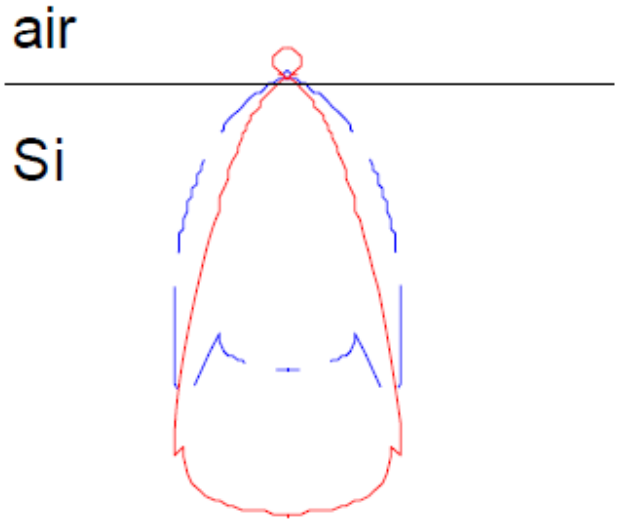

(b)

Optical absorption (1-R-T) in Si wafers

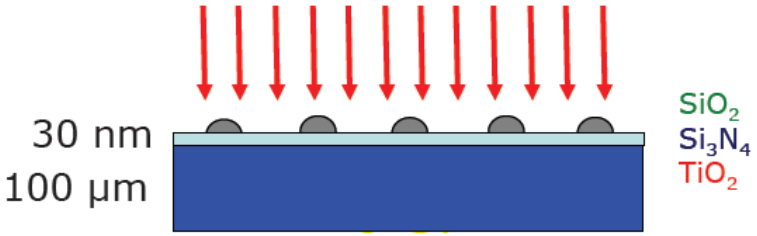

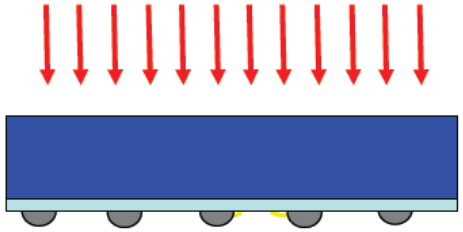

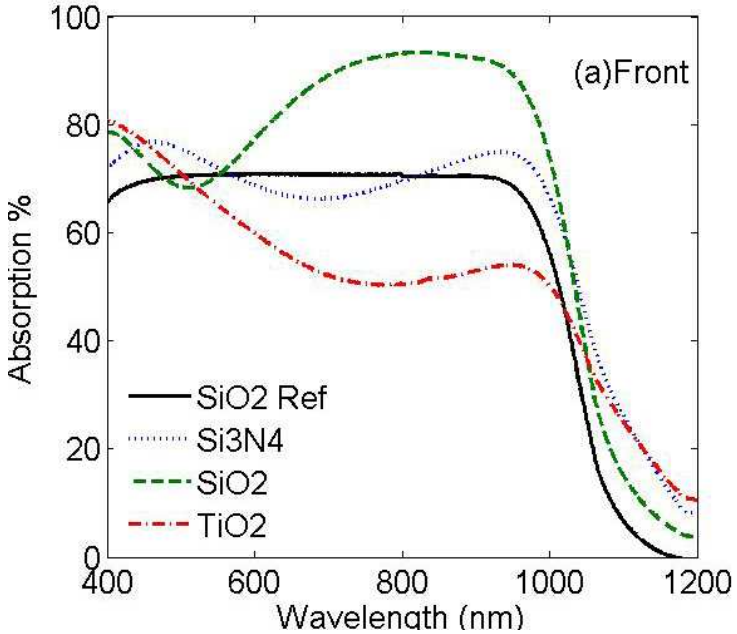

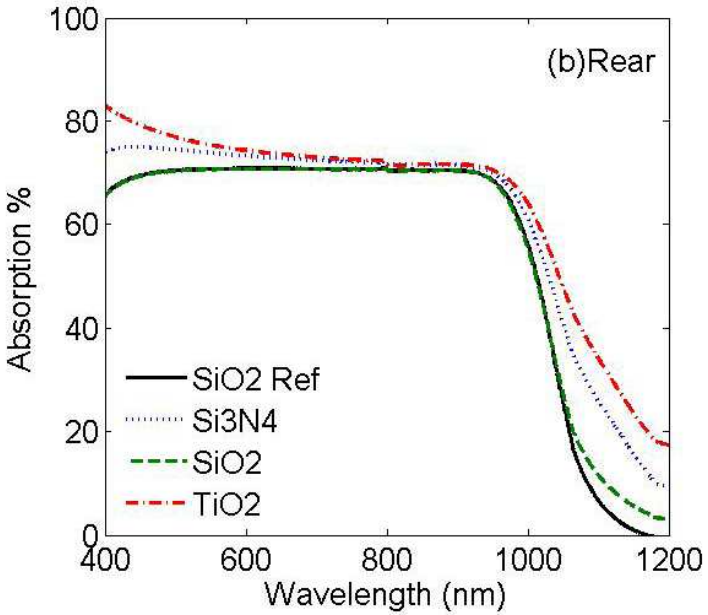

Kylie Catchpole, Fiona Beck
J. Appl. Phys. **105, 114310 (2009)**

Plasmonic solar cells

Extinction (solid lines) and scattering (dashed lines) cross-sections for 100-nm diameter Ag spheres embedded in air (black), Si3N4 (*n=2, blue) and Si (red), normalized by the projected* area of the sphere. The dipolar resonance for Si peaks at 1190 nm and is outside the range of the graph.

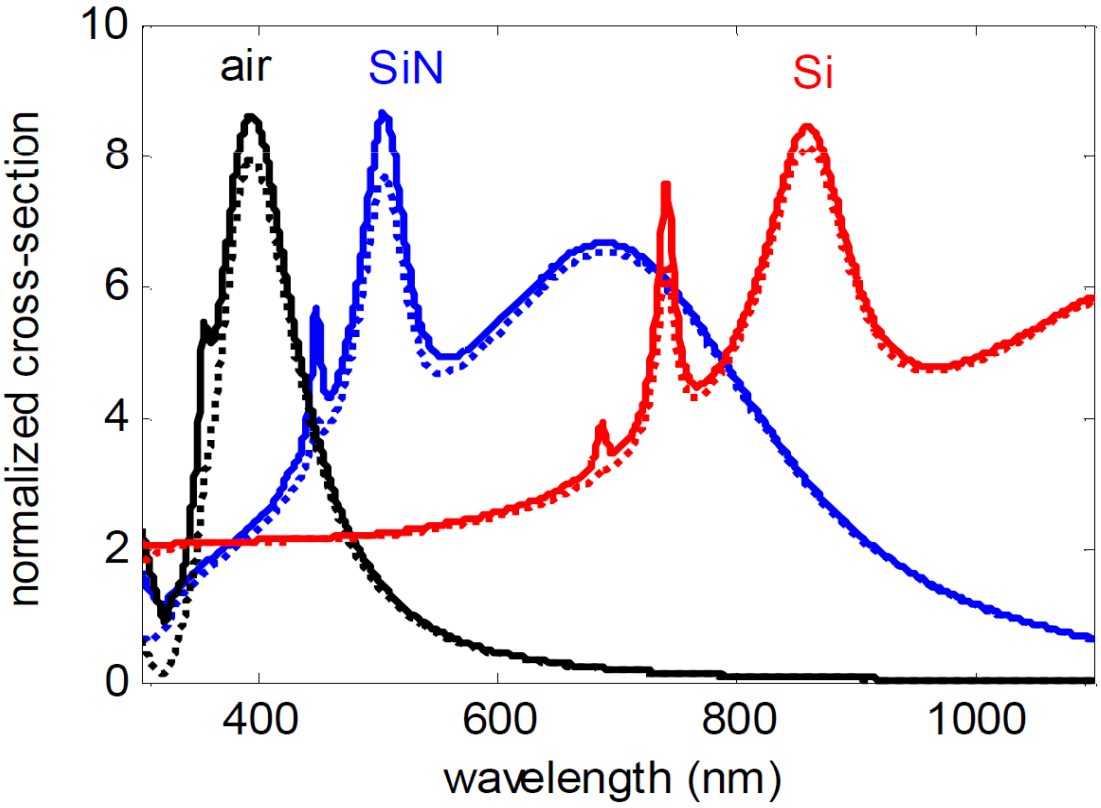

M. Green et al.,
"Annual Report April 2010,

Fabrication of large-area metal nanopatterns

Evaporation and annealing (ANU)

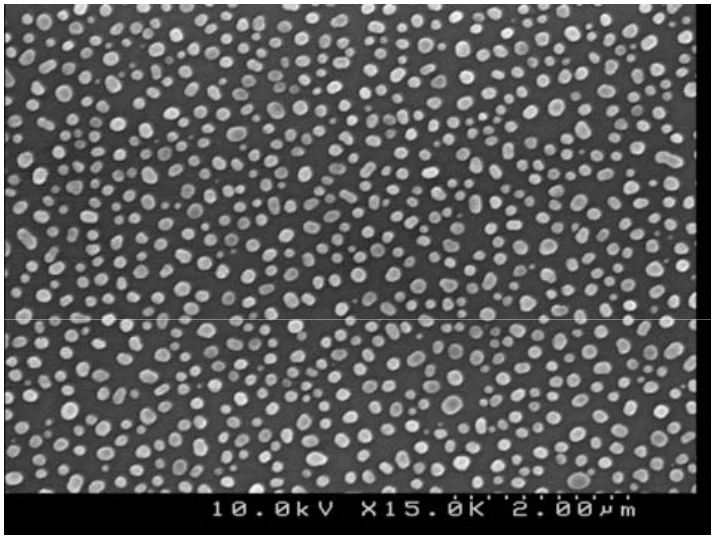

Porous alumina template (CALTECH)

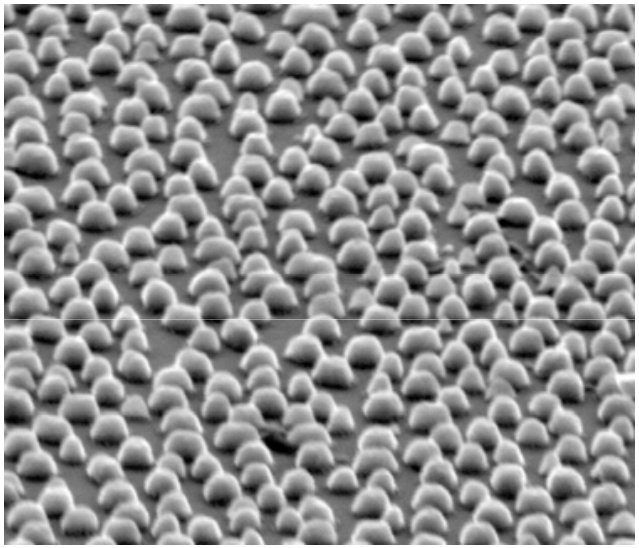

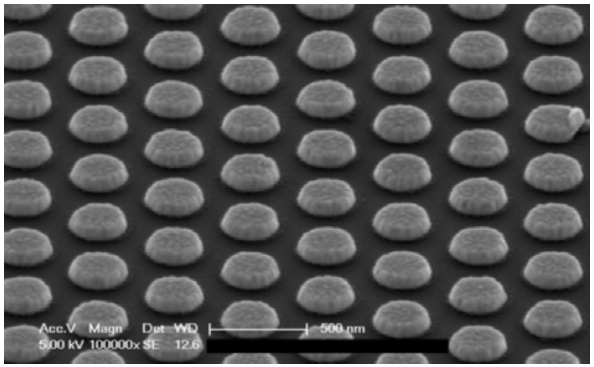

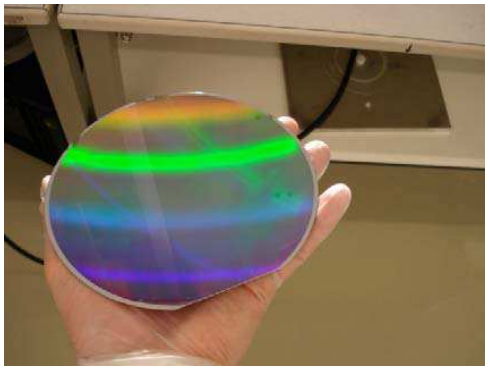

Substrate conformal imprint lithography (SCIL) -Philips

Improvement of energy conversion efficiency of amorphous silicon thin-film solar cells through plasmon effect

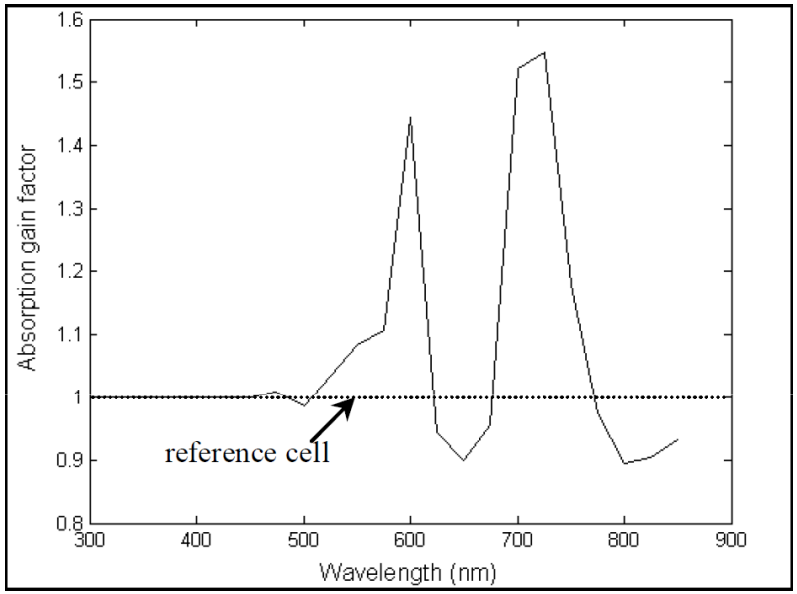

Gain in Si absorption vs wavelength using 20nm Ag nanoparticles relative to reference cell.

M. Green et al.,
"Annual Report April 2010,

Langmuir-Blodgett (LB) deposition of nanoparticles

The LB technique allows for the formation of ordered monolayers at an air-water interface using whilst exploiting the self-organization mechanism of colloidal dispersion. Compression of the monolayer is monitored via measurements of surface pressure (SP), see Figure 9. This reaches a maximum at the highest density of nanoparticles in the plane, corresponding to a highly organized 2D crystal structure.

Schematic diagram of the LB apparatus

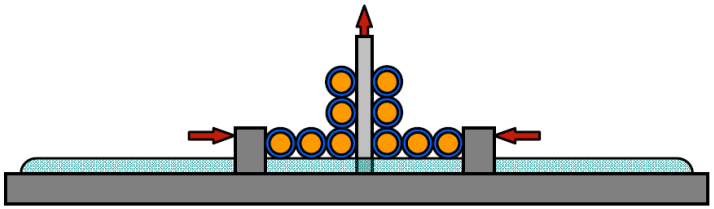

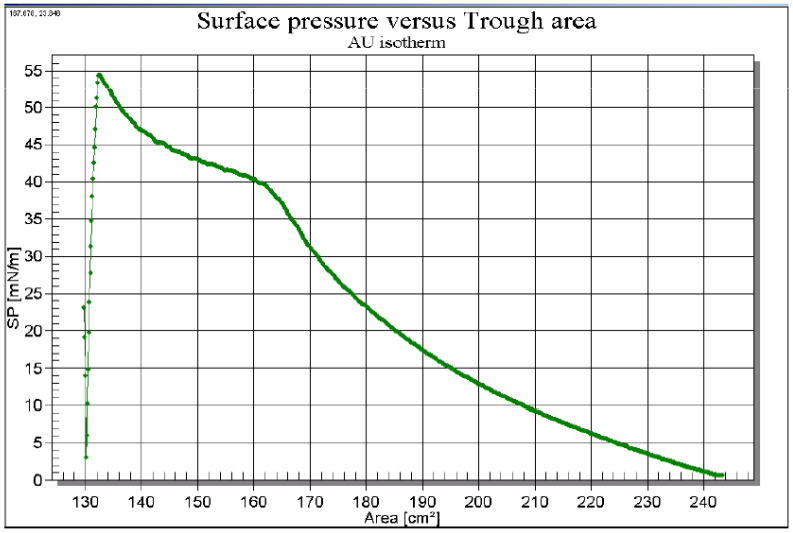

Surface pressure isotherm of Au nanoparticle on the water surface. The maximumSP, of 55mN/m at 132cm2, corresponds to the maximum packing in the plane and a high degree of 2D crystallinity.

Fabrication of Si quantum dots

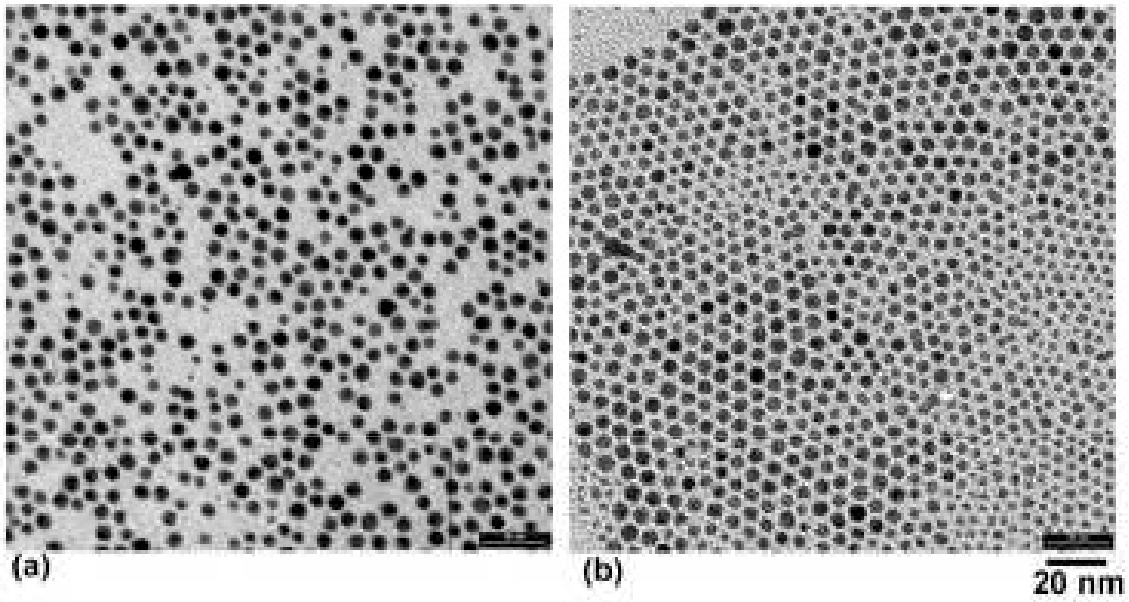

TEM images of Au nanoparticle onolayers deposited at surface pressures of 20 mN/m (a) and 30 mN/m (b).

M. Green et al., “Annual Report April 2010, ARC Photovoltaics Centre of Excellence at the University of New South Wales

Silicon multiple exciton generation/pn junction hybrid solar cell; Sean Jacobs, 33 rd PVSC

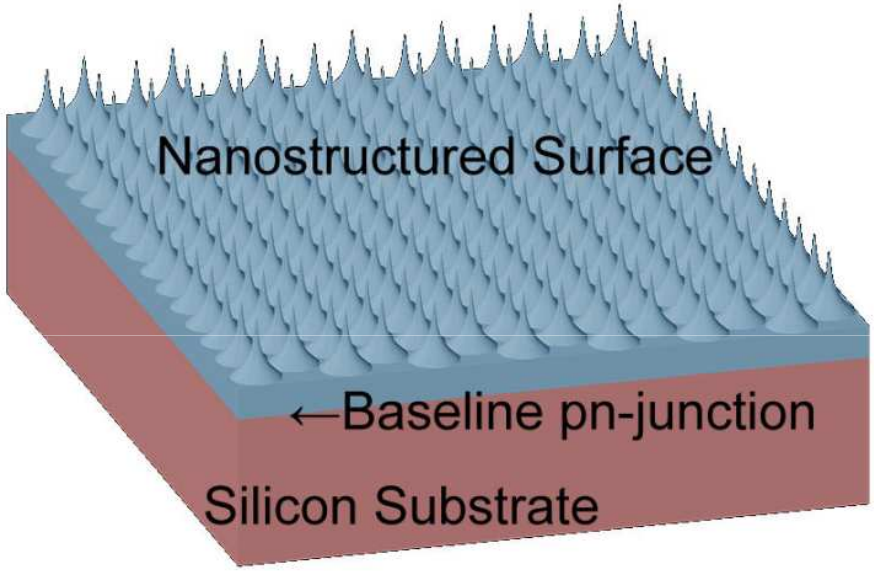

Limit wydajności ogniwa przy 1 Sun zwiększa się z 30% do 42% gdy M ≥ 4 dla E_g = 1.1 eV.

$$Q(E_{ph}) = \begin{cases} 0 & 0 < E_{ph} < E_g \\ m & mE_g < E_{ph} < (m+1)E_g \quad m = 1,2,3 \ldots \\ M & E_{ph} \geq ME_g \end{cases}$$

Band diagram of a Hot Carrier solar cell

Hot carrier absorbers slowing of carrier cooling.
GaN, InN, InP

Energy selective contact base on double barrier resonance tunneling to the energy levels in QD layer between two dielectrics (conductance sharply peaked on the hot absorber side)

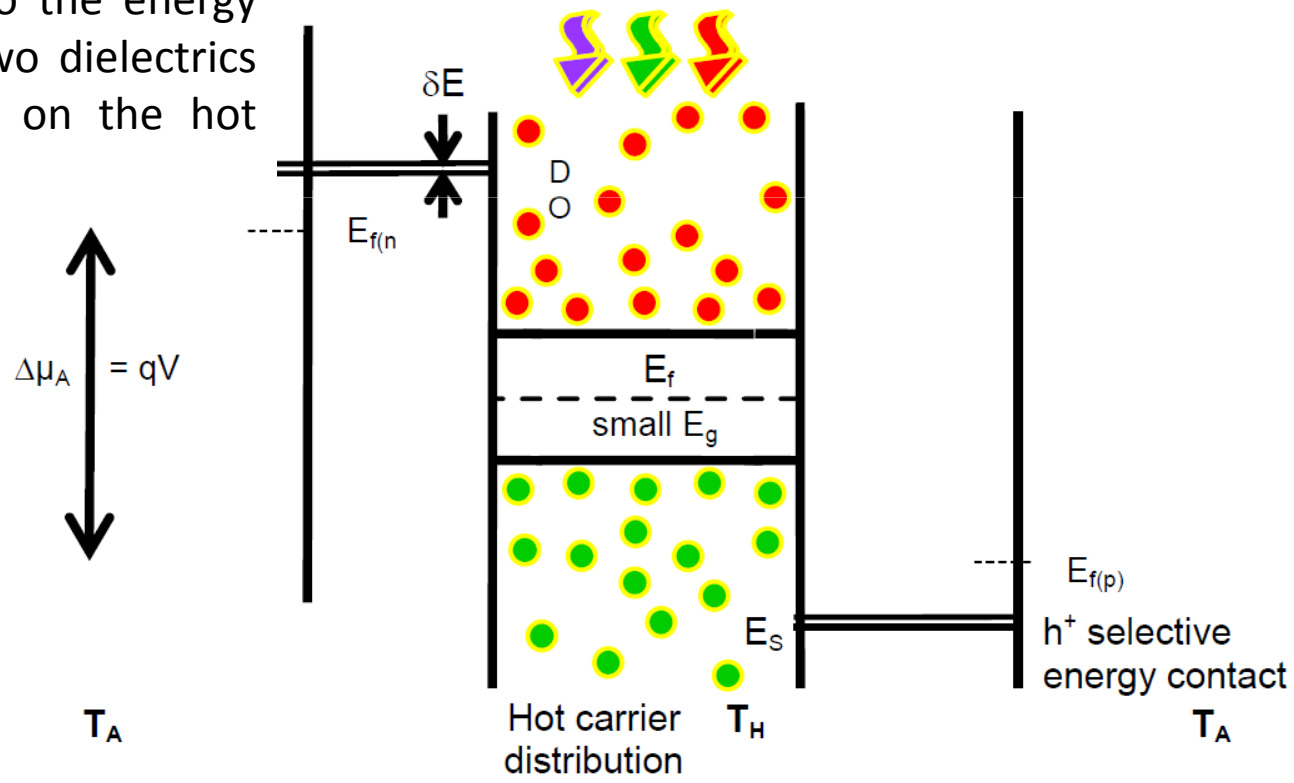

M. Green et al., "Annual Report April 2010 ,

Compounds for Hot Carrier solar cell

Ratios of phononic band gap energy values for various binary compounds:
■ & □ energy gap between acoustic and optical modes normalised to acoustic frequency; ▲& Δ energy dispersion of optical modes. Filled Symbols (■ &▲) refer to DFT calculations of diatomic 'molecules' fed into a 1D diatomic chain model whereas Open Symbols (□ &Δ) refer to calculations based on simple elemental masses. The dashed line indicates the point at which the phononic gap equals the maximum acoustic phonon energy.

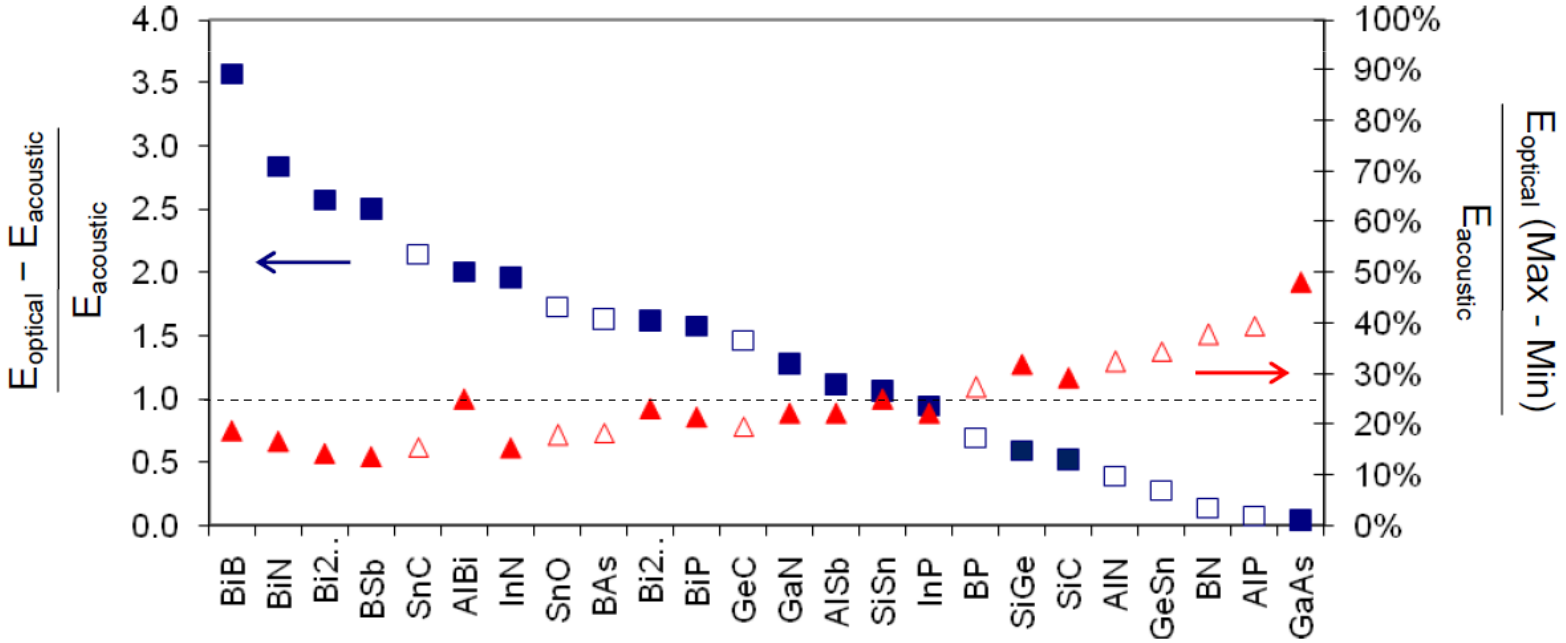

M. Green et al., "Annual Report April 2010 ,

Zastosowanie wybranych efektów kwantowych

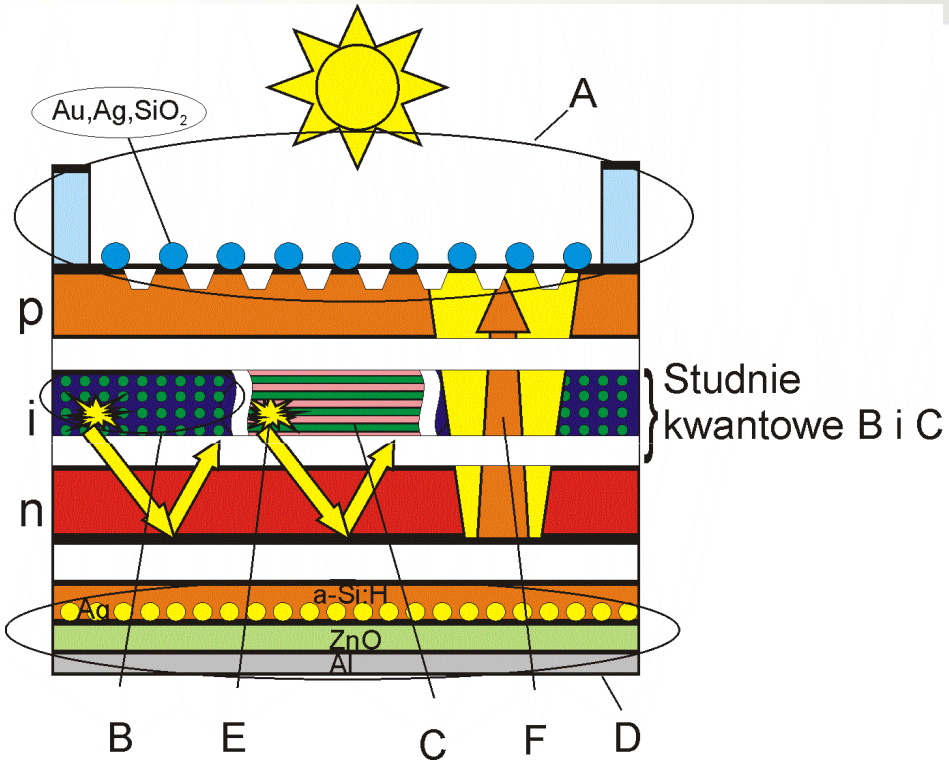

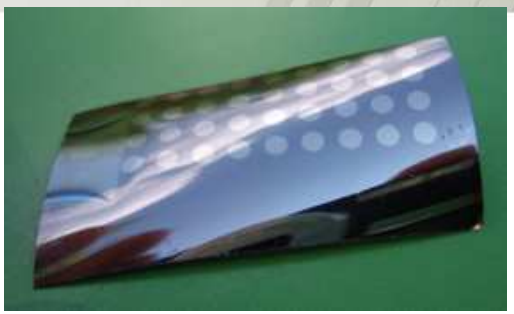

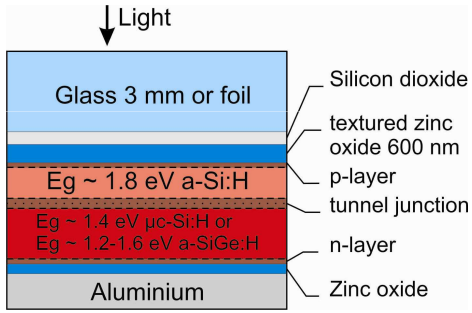

Schemat proponowanej struktury ogniwa słonecznego

A - Nanoteksturyzowana elektroda frontowa,

B - Warstwa amorficznego krzemu z jednorodnie rozmieszczonymi nanokryształami Si,

C - Studnie kwantowe typu a-Si:H/a-Ge:H lub a-Si:H/µc-Si:H,

D - Elektroda tylnia w formie lustra Bragg'owskiego,

E - Foton z rekombinacji promienistej odbijanej od elektrody "D",

F - niezaabsorbowane fotony odbijane od elektrody tylniej

Zastosowanie wybranych efektów kwantowych

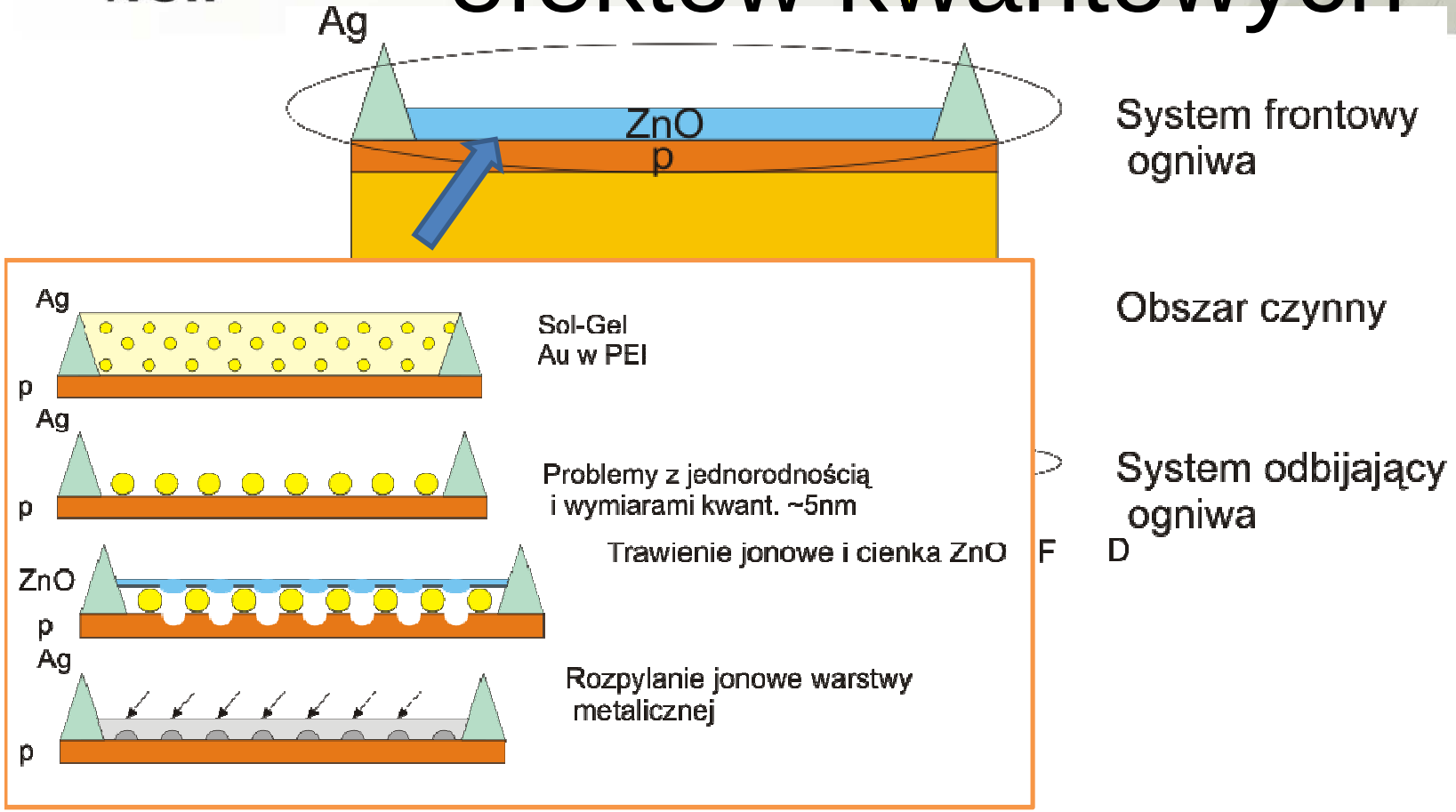

Fabrication of Si quantum dots

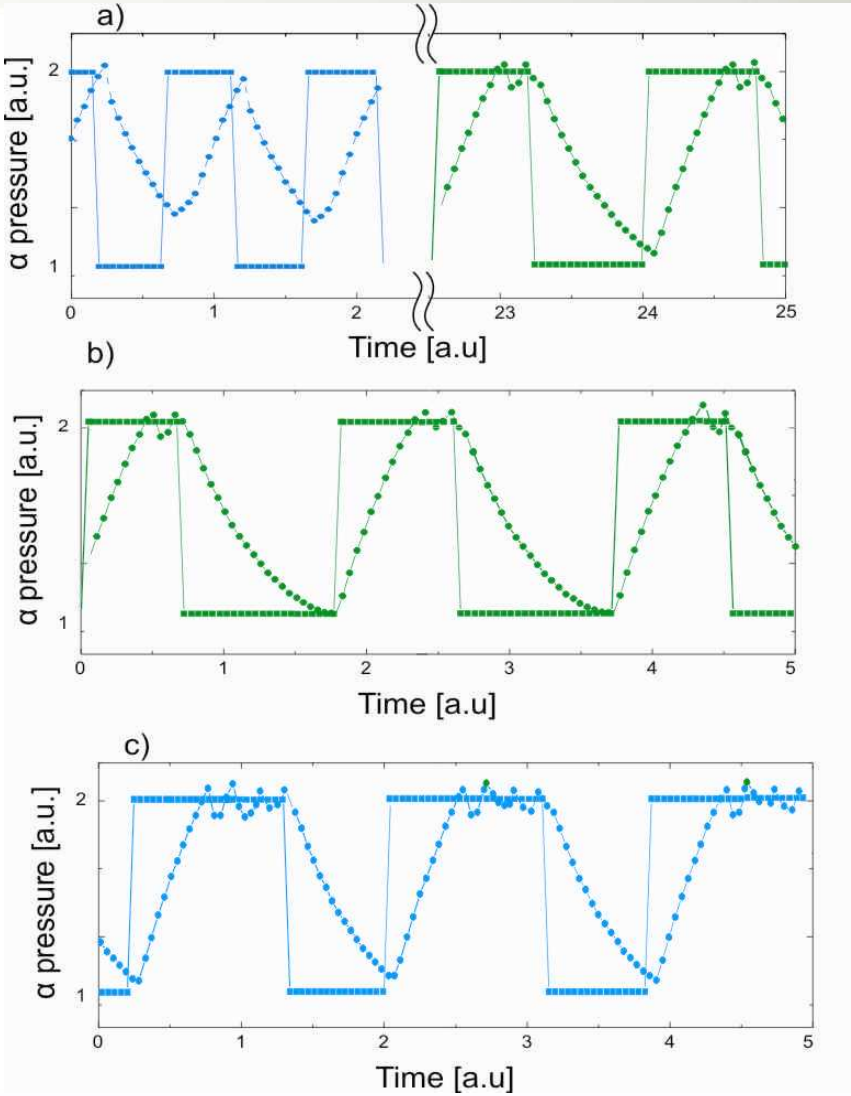

Fabrication of Si quantum dots Results

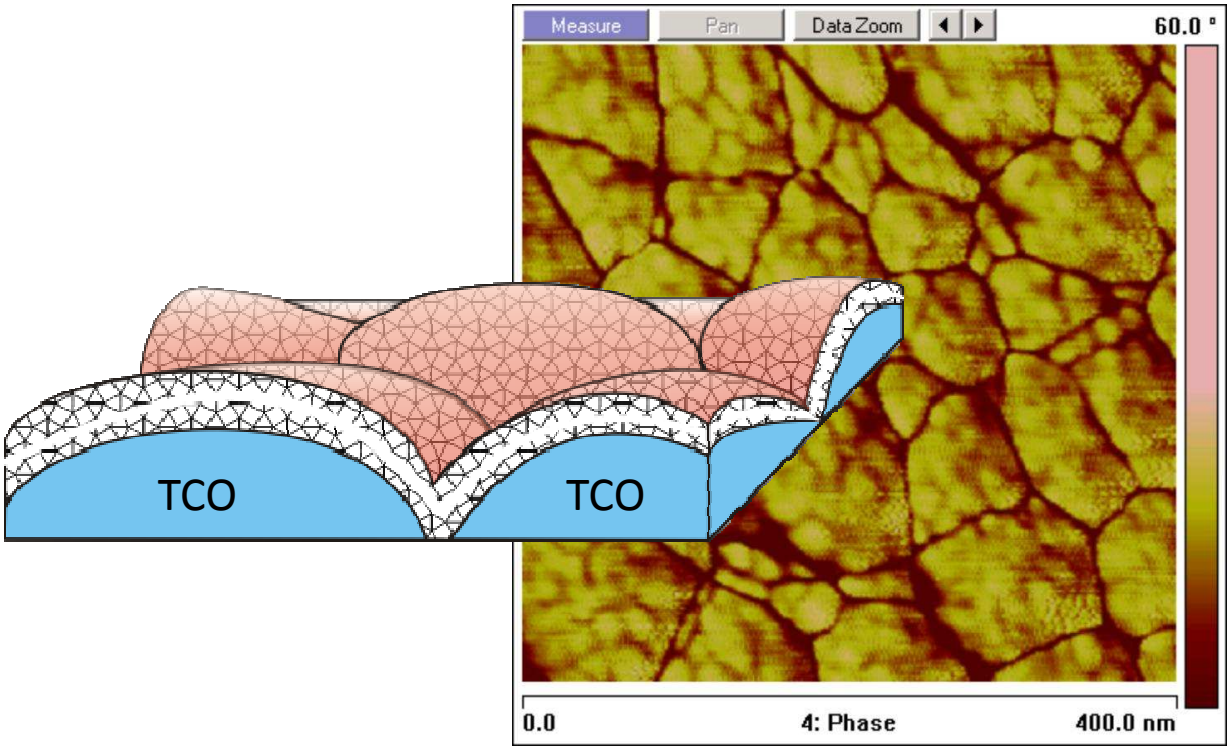

Exemplary phase ATM pictures of multilayer structure 240 double a_2 cycle by MS technique nc –Si:H layer. It is seen stress form substrate caused big complexes and inside them a small Si crystallites can be indicated on 8 – 12 nm (corresponding image gives rms 3,69 nm).

X ray measurements of QD Structure

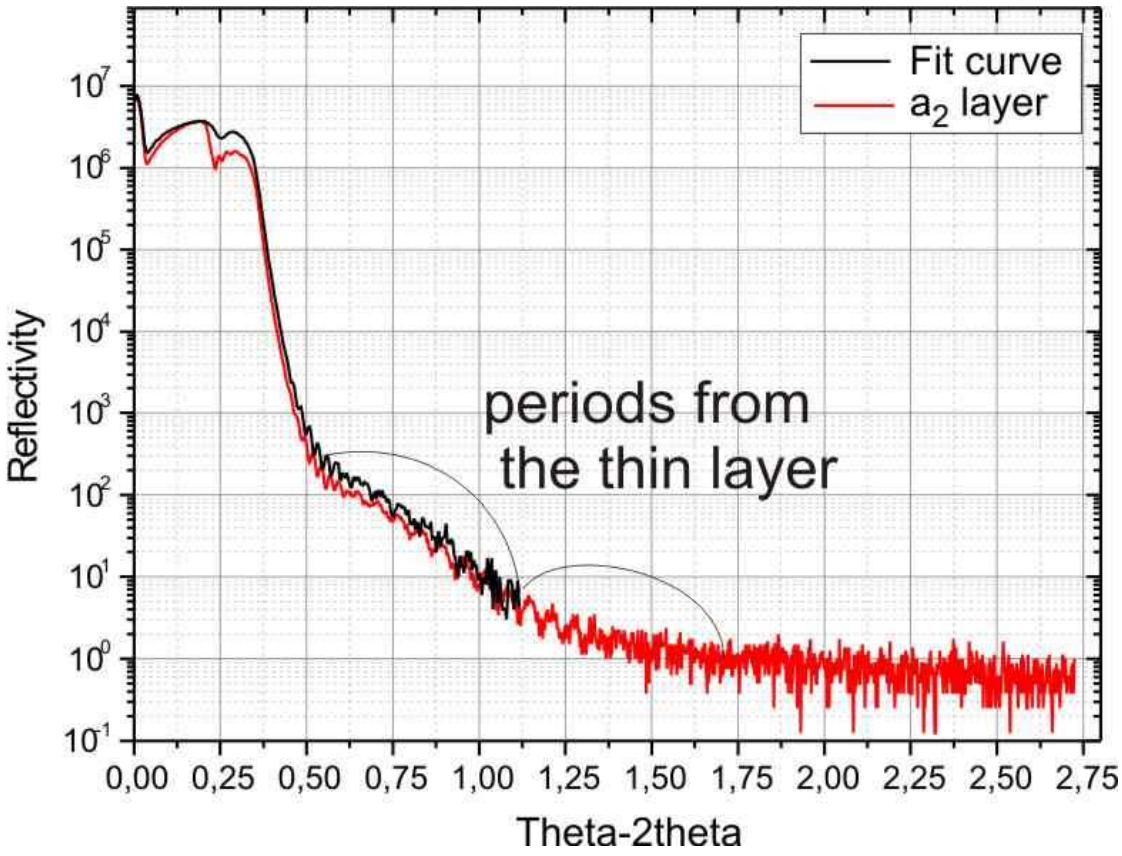

X ray reflectivity curve and theoretical fit for the film a_2 made during 240 cycles shown in Fig. 6. with assumption that substrate TCO is 150 nm and the period for Si film is 6nm.

Optical Measurements of QD structure

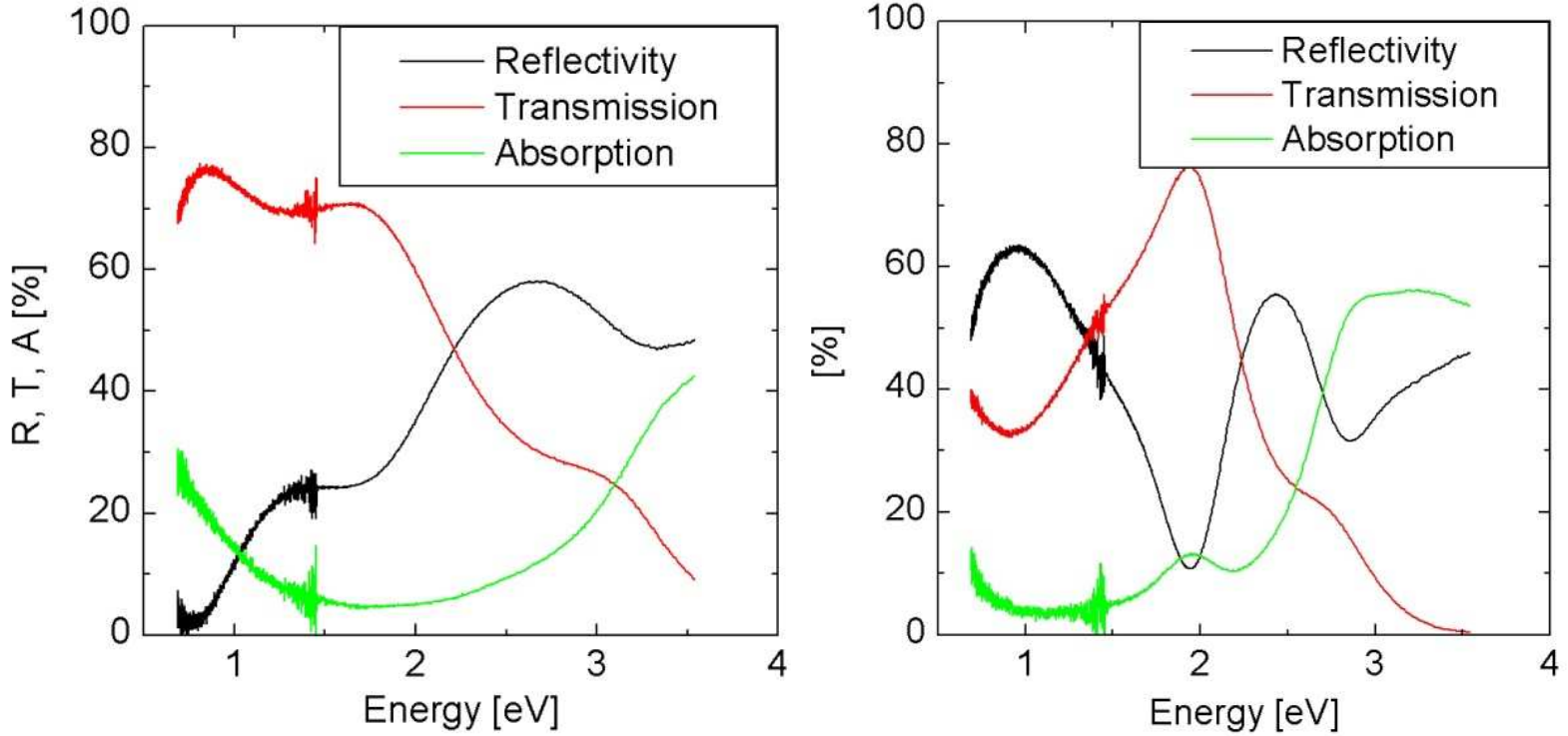

Exemplary shown difference in absorption between multilayered amorphous (a) and nanocrystalline (b) layers thick 0.15 µm deposited on ITO. Calculated from the above curves energy gap E_g equal for a_1 and $a\text{-}_2$ structures 1,76 eV and 1,42eV respectively

.

Diagram of the deposited structure a-Si:H and a-Si:H/ µc-Si:H by RF PECVD in the multistep technology

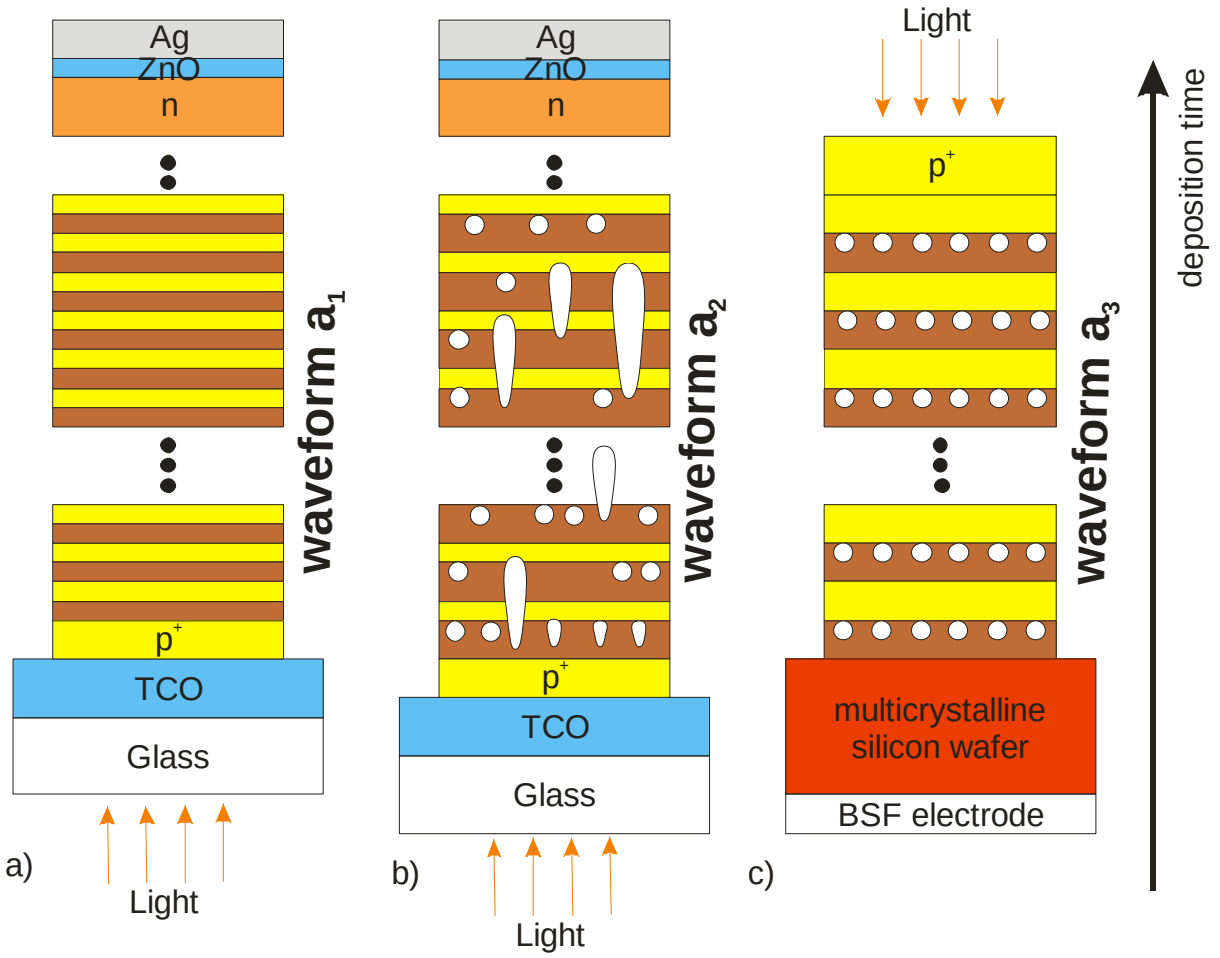

MODELING OF SILICON QUANTUM DOTS FOR SOLAR CELL APPLICATIONS; M. M. Adachi 34 PVSC

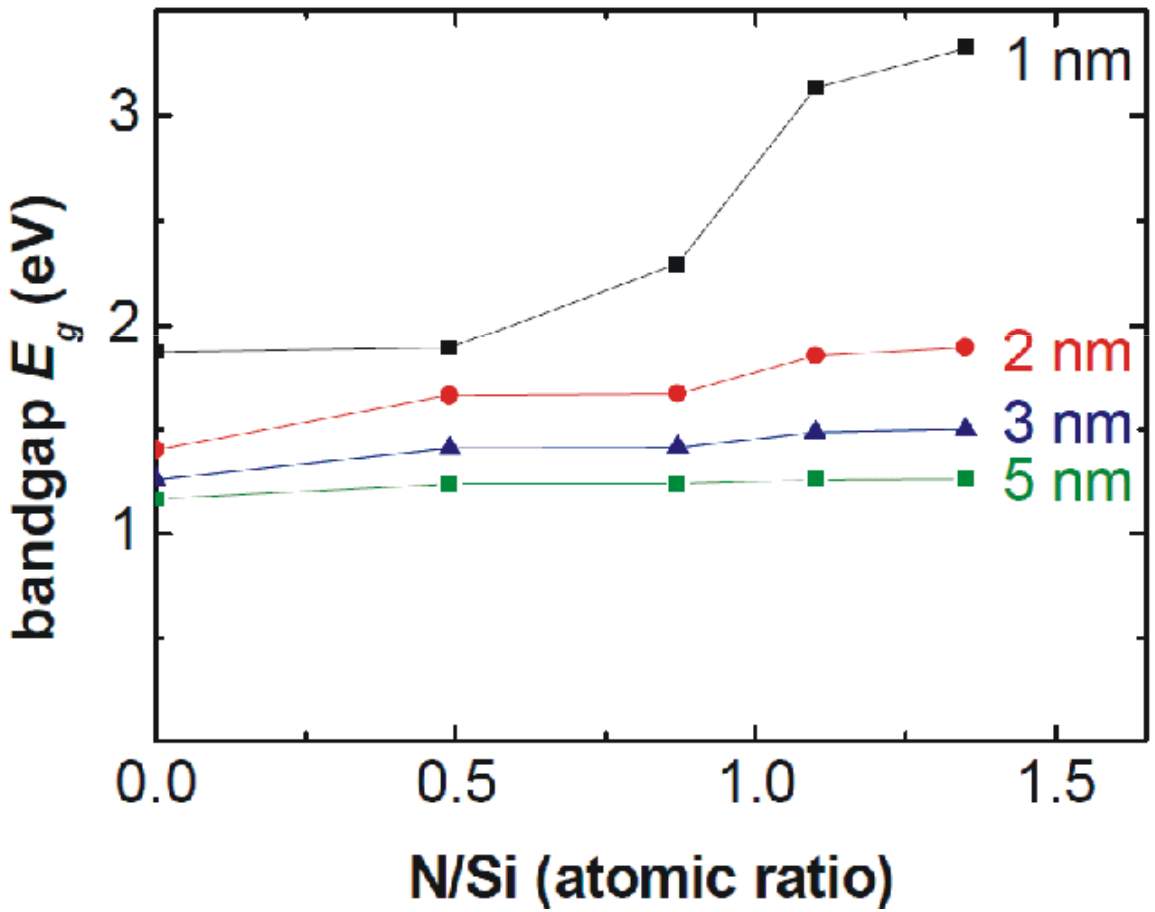

Zastosowanie wybranych efektów kwantowych

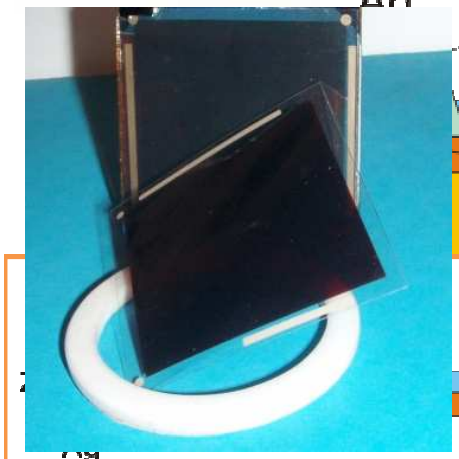

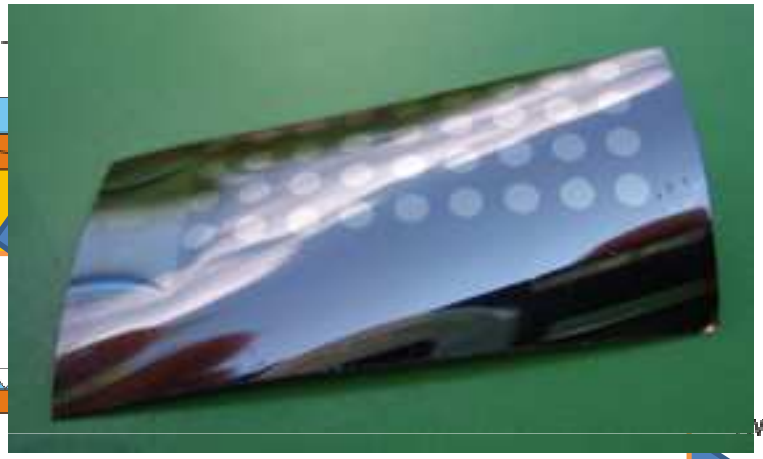

System frontowy ogniwa

Obszar czynny

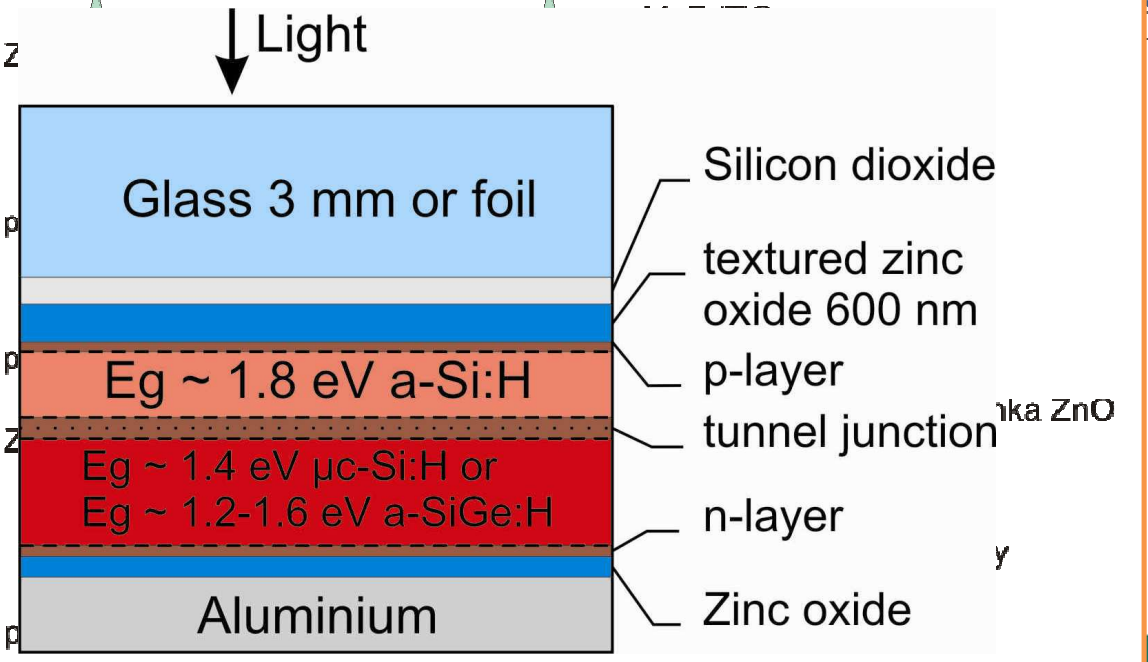

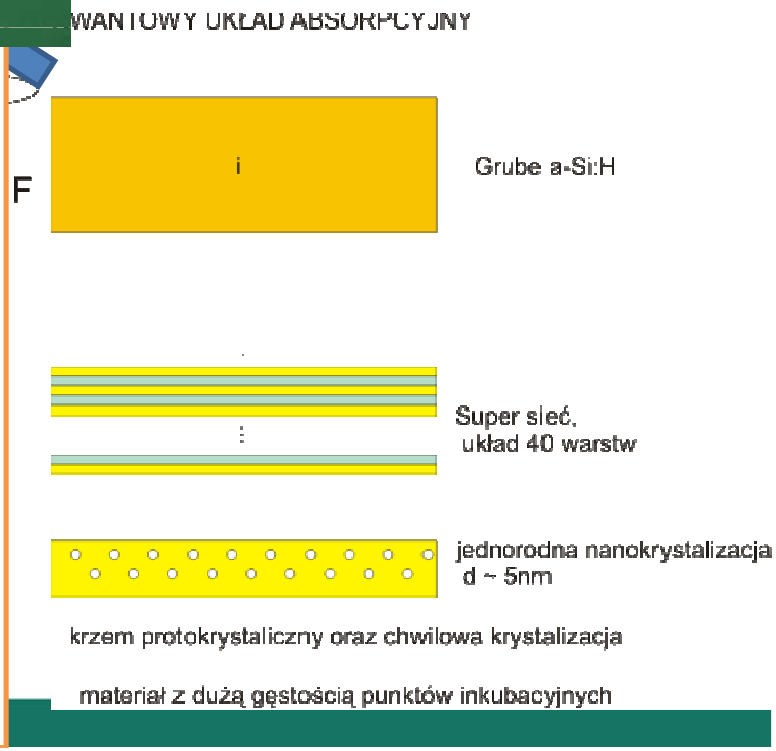

Photocurrent, external quantum efficiency

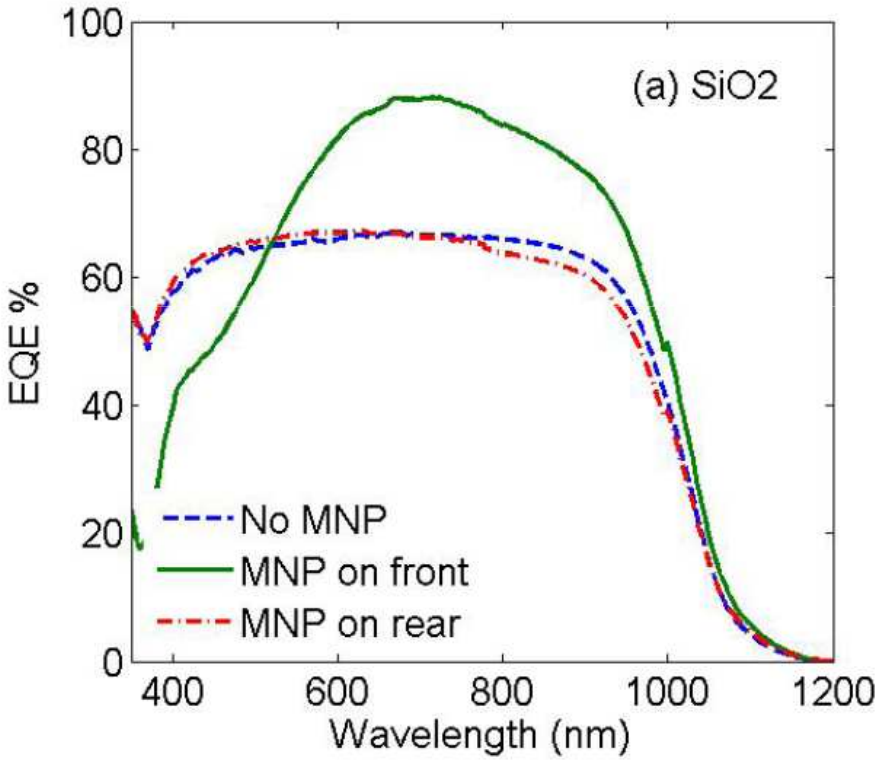

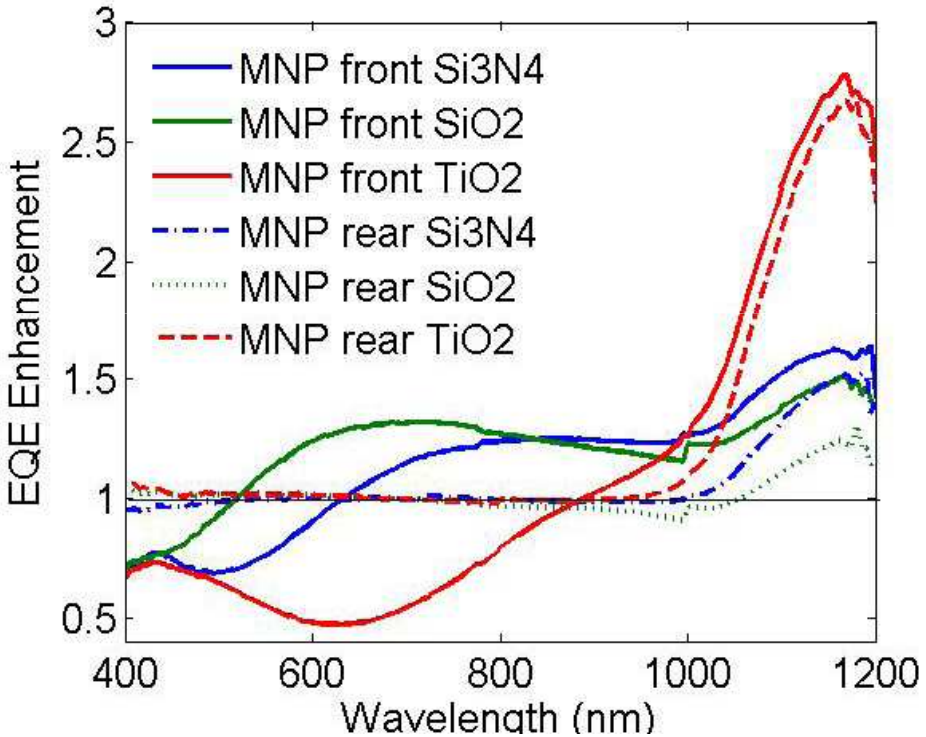

Kylie Catchpole, Fiona Beck
J. Appl. Phys. **105, 114310 (2009)**